Hindawi
Advances in Polymer Technology
Volume 2020, Article ID 8976713, 7 pages
https://doi.org/10.1155/2020/8976713

Research Article

Effect of Oxidized Wood Pulp Fibers on the Performance of the Thermoplastic Corn Starch Composites

Peng Yin,[1] Wen Zhou,[1] Xin Dong,[1] Bin Guo ,[1,2,3] and Yanan Huang[2,3]

[1]*College of Science, Nanjing Forestry University, Nanjing 210037, China*
[2]*Agricultural and Forest Products Processing Academician Workstation, Luohe 462600, China*
[3]*Postdoctoral Research Center of Nanjiecun Group, Luohe 462600, China*

Correspondence should be addressed to Bin Guo; gbm@ustc.edu

Received 17 April 2020; Accepted 16 June 2020; Published 8 July 2020

Academic Editor: Coro Echeverria

In this study, oxidized wood pulp fiber (OWPF) was prepared by oxidizing wood pulp fiber (WPF) with $NaIO_4$, and OWPFs with different oxidation degrees were obtained and characterized by light microscope, XRD, and TG. Then, OWPFs with different oxidation degrees were incorporated into thermoplastic starch (TPS) to prepare OWPF/TPS composites. The cross-section morphology, water resistance, and physical and mechanical properties of the composites were investigated. SEM showed good dispersion of OWPF in the continuous TPS phase. The tensile strength of OWPF/TPS reached a maximum value of 5.02 MPa when the oxidation degree of OWPF was 0.5. Elongation at break of OWPF/TPS composites increased with the increasing oxidation degree of OWPF. Meanwhile, as a result of cross-linking, the water contact angle was also improved with the increased oxidation degree of OWPF. The study provided a new way to prepare a degradable TPS composite with satisfying properties to be used for packaging and catering.

1. Introduction

In recent years, great attention has been paid to thermoplastic starch (TPS), which is considered as the most promising biodegradable plastic due to its low-cost, ample supply of starch from renewable sources, and totally degradable properties [1]. However, its broader application is limited by two major deficiencies, namely, poor mechanical properties and pronounced sensitivity to moisture [2].

One of the most important methods to overcome the abovementioned problems is to add reinforcements to TPS. As is well known, organic fibers and inorganic mineral materials are two major kinds of reinforcements. Natural fibers such as cotton fiber [3], flax fiber [4], coir fibers [5], luffa fiber [6], and inorganic mineral materials including montmorillonite [7], kaolinite [8], halloysite [9], and rectorite [10] had been added to TPS to improve mechanical and water-resistant properties.

Up to now, many researches have focused on the investigation of organic fiber-reinforced TPS. Results showed that the property improvement depends on several factors such as adding dosage, aspect ratio, and dispersion condition of the fibers. Among these factors, dosage of the fibers is a main factor which often affects the mechanical properties of TPS. For example, it was found in Ma's [11] study that when the fiber content was increased from 0 to 20 wt%, the initial tensile strength of TPS was trebled up to 15.16 MPa. The shape and size of the fibers are also important factors which affect the mechanical and thermal stability properties. Short fibers have a higher specific surface area which leads to greater stress at maximum load [12], while long fibers are effective for enhancing thermal stability [13]. The dosage and shape and size of the fibers also affect their dispersion in the TPS matrix. Homogeneous dispersion of the fibers is favorable for the improvement of mechanical property, e.g., a glycerol-plasticized pea starch/MCC (microcrystalline cellulose) composite showed good mechanical properties because of the excellent dispersion of MCC [14]. Cross-linking between the matrices is often a useful method to improve TPS's properties, especially the water-resistant property. In Iman and Maji's study [15], glutaraldehyde was used as a cross-linker which could react with the starch

and improve the water resistance and mechanical properties of TPS effectively. In Zhou et al.'s [16] study, nanocellulose fibers modified by oxidation showed excellent dispersion in a PVA matrix, resulting in superior tensile modulus and strength of the composites. Cross-linking may have occurred between nanocellulose and PVA.

In this study, oxidized wood pulp fiber (OWPF) was prepared by oxidizing wood pulp fiber (WPF) and using it as a reinforcement to prepare OWPF/TPS composites. The goal is to make OWPF not only as a reinforcement but also as a cross-linker in the TPS matrix. The effects of different oxidation degrees of OWPF on the properties of WPF and the morphology, mechanical properties, thermal properties, and surface wettability of OWPF/TPS composites were investigated in detail.

2. Materials and Methods

2.1. Materials. Corn starch was supplied by the Shandong Hengren Industry and Trade Company (Tengzhou, Shandong, China). Bleached softwood pulpboard was supplied by the Shandong Dawnsen New Material Co. Ltd. (Longkou, Shandong, China). Glycerol, glycol, methanol, and sodium hydroxide, as analytical reagents, were purchased from Sinopharm Chemical Reagent Co., Ltd. (Shanghai, China). Sodium periodate, as an analytical reagent, was purchased from Shantou Xilong Chemical Plant Co., Ltd. (Shantou, Guangdong, China). Chloride hydroxylamine, was purchased from Shanghai No. 4 Reagent & H. V. Chemical Co., Ltd. (Shanghai, China). Sulfuric acid,was a chemically pure reagent and purchased from Nanjing Chemical Reagent Factory (Nanjing, Jiangsu, China).

2.2. Preparation of WPF and OWPF. Firstly, a piece of softwood pulpboard was cut into small pieces, then softwood pulpboard (50 g) and 15 wt% NaOH (300 mL) were added into the beaker in order to wet the softwood pulpboard completely. In fact, it is a process of swelling and activation for the pulpboard. At the same time, small impurities in the pulpboard were also removed in this process. After 5 h, HCl was added rapidly to neutralize NaOH. Then, the deposit was filtered by a sand-cored funnel and washed with distilled water to pH 7.0. The WPF was obtained after drying at 50°C for 8 h.

WPF and 60 wt% H_2SO_4 (150 mL) were added into a 500 mL beaker for hydrolysis reaction at 45°C for 0.5 h under stirring, then the slurry was washed with distilled water repeatedly at 3000 rpm to remove acids and other small molecules. The deposit was dried by a freeze-dryer.

The sodium periodate solution (250 mL) was added into a 500 mL flask in a water bath at constant temperature (50°C) and then adjusted to pH 4.0. 20 g WPF was added rapidly into the flask for a dark thermostatic reaction for 3 h under stirring, and ethylene glycol (50 mL) was added to remove unreacted sodium periodate for 1 h. The suspension was filtered, repeatedly washed with distilled water, and dried.

2.3. Determination of Aldehyde Group Content. The aldehyde contents of OWPF are determined using the hydroxylamine hydrochloride method according to Yu et al.'s study [17] based on the following chemical reaction:

$$-\mathrm{CHO} + NH_2OH \cdot HC1 \longrightarrow -CHNOH + H_2O + HC1 \quad (1)$$

The released HCl was titrated with a sodium hydroxide-methanol solution during the reaction in methanol. OWPF (0.5 g) was added in hydroxylamine hydrochloride (10 mL of 0.05 g/mL) solution. The pH was adjusted to 5.0 with NaOH (0.1 mol/L) solution. The conversion of aldehydes into oximes continued at 40°C for 4 h. The aldehyde content was determined using equation (2) by recording the consumption V_1 (mL) of NaOH (0.1 mol/L), performing the reaction at a constant pH of 5.0. 0.5 g WPF without oxidation was used as a control to record the consumption V_2 (mL) of NaOH.

Aldehyde content is calculated as

$$\mathrm{CHO}\,(\%) = \frac{M(\mathrm{CHO}) \times c \times (V_1 - V_2)}{m \times 1000} \times 100, \quad (2)$$

where M (CHO) is the molar mass of the –CHO group (29 g/mol); c is the concentration of NaOH (0.1 mol/L); V_1 is the volume of the consumption of NaOH for OWPF (mL); V_2 is the volume of the consumption of NaOH for WPF without oxidation (mL); m is the mass of OWPF or WPF (0.5 g).

2.4. Preparation of OWPF/TPS Composites. Glycerol was blended with corn starch and OWPF by the High-Speed Mixer (GH-100Y, China) and then stored overnight. The ratio of glycerol and corn starch (w/w) was 1 : 3 (100 g, 300 g). The OWPF loading level (6 wt%) was based on the amount of TPS. The mixtures were manually fed into a twin screw plastic extruder operating at 150 rpm. The temperature profile along the extruder barrel was based on four heating zones, which were 115, 120, 125, and 115°C from the feed zone to the die. The die has a hole of 3 mm in diameter. Samples were cut into small particles by a pelletizer. Dumbbell-shaped specimens (ASTM D638) were made from these small particles by injection molding. The scheme of the cross-linking reactions between OWPF and starch is shown in Figure 1.

2.5. Light Microscope. A light microscope (MA1000/MA2000, Chongqing Optical Instrument Co., Ltd, China) was used to observe the morphology of WPF and OWPF with different degrees of oxidation, and the resolution of the light microscope was 1.0 μm.

2.6. X-Ray Diffractometry. X-ray diffraction patterns were recorded in the reflection mode in an angular range of 5-60° (2θ) at ambient temperature by an X-ray diffractometer (Ultima IV, Rikagu, Japan). Radiation was operated at 30 kV and 30 mA.

2.7. Thermal Stability. TG thermograms and DTG of a sample were recorded by a thermogravimetric analyzer (TG 209 F1, NETZSCH, Germany). Samples were tested under a nitrogen atmosphere within a temperature range of 50–600°C at a heating rate of 20°C/min.

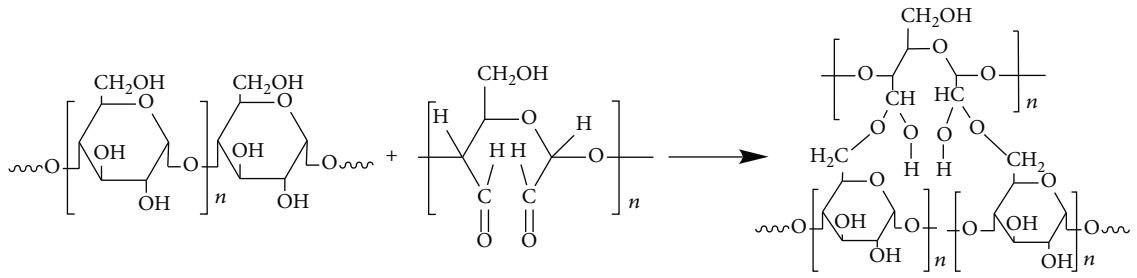

Figure 1: Schematics of cross-linking reaction between OWPF and TPS.

Table 1: The aldehyde contents of OWPF prepared at the different ratios of m($NaIO_4$)/m(WPF).

Sample no.	Hydrolysis temperature (°C)	Reaction temperature (°C)	Reaction pH	m($NaIO_4$)/m(WPF)	CHO (%)
1	45	50	4.0	0.125	1.624
2	45	50	4.0	0.250	2.387
3	45	50	4.0	0.375	4.640
4	45	50	4.0	0.500	5.510

2.8. Scanning Electron Microscopy (SEM). The fracture surfaces of OWPF/TPS composites were examined using a field emission scanning electron microscope (JEOL JSM-7600F, Japan). The fracture surfaces were vacuum-coated with gold for SEM, which were fractured in tensile tests.

2.9. Mechanical Testing. Tensile tests were conducted according to ISO 527-2012 at a temperature of 20 ± 2°C and relative humidity of 55 ± 5%. The tensile measurements from dumbbell specimens were carried out using Testing Medicine (SANS, Shenzhen, China) with a cross-head speed of 20 mm/min. It should be noted that the results of the mechanical properties of the samples were obtained by averaging from 5 independent tested specimens.

2.10. Contact Angle Measurement. OWPF/TPS composites were measured with a contact angle testing instrument (DSA100, Kruss, Germany). It should be noted that the contact angle testing results of the samples were obtained by averaging from 10 independent tested specimens, and the contact angle was tested 20 seconds after the water droplets fell into the specimen.

3. Results and Discussion

3.1. Characterization of OWPF

3.1.1. Aldehyde Contents and Morphology of OWPF. Table 1 lists the aldehyde contents of OWPF, which are prepared at the conditions of different mass ratios of $NaIO_4$/WPF. It can be seen that aldehyde contents of OWPF increased with the increase of m($NaIO_4$)/m(WPF) under the same hydrolysis temperature, reaction temperature, and pH conditions. When the ratio of m($NaIO_4$)/m(WPF) is 0.5, the aldehyde contents reached 5.5%.

The morphology of WPF before and after oxidation was observed by a polarizing microscope (100x). As shown in Figures 2(a) and 2(b), hydrolysis made the fibers shorter and more dispersed. But after oxidation, the fibers became rod-like and the phenomenon of birefringence became more obvious (Figures 2(c)–2(f)). This can be due to the breakdown of the amorphous region of the fibers during oxidation. The aspect ratio of the fibers decreased with the increase of the oxidation degree. When the ratio of oxidant m($NaIO_4$)/m(WPF) reached 0.5 and the aldehyde contents of the fibers reached 5.5%, the length of OWPF was below 100 μm (Figure 2(e)).

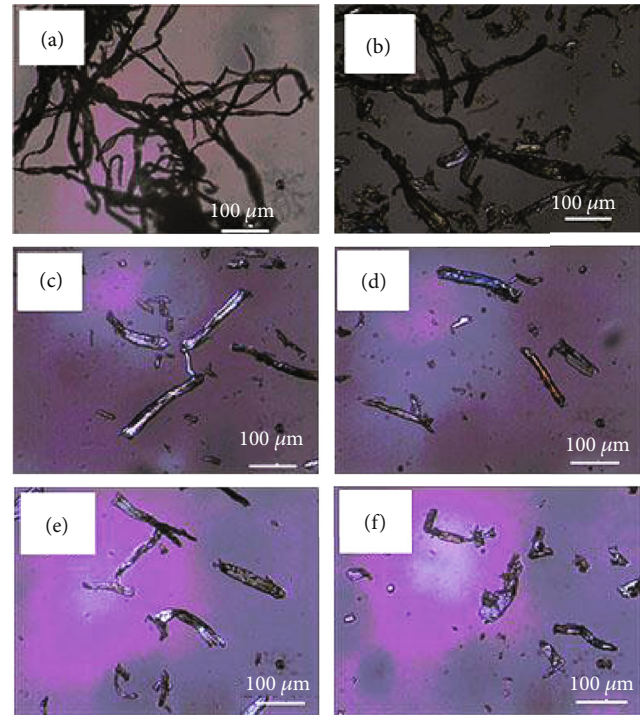

Figure 2: Polarizing microscope micrograph (100×) of WPF before and after hydrolysis and OWPF with different oxidation degrees: (a) before hydrolysis; (b) after hydrolysis (0); (c) 0.125 OWPF; (d) 0.25 OWPF; (e) 0.375 OWPF; (f) 0.5 OWPF.

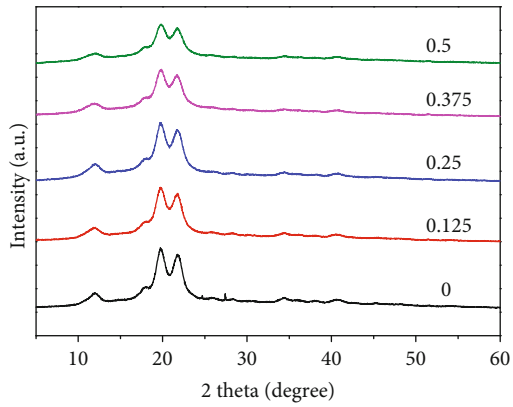

Figure 3: XRD spectra of OWPF with different degrees of oxidation.

3.1.2. X-Ray Diffractometry. The effect of oxidation on the crystalline structure of WPF was investigated by X-ray diffraction (XRD) analysis. XRD patterns of WPF and OWPF are shown in Figure 3. Obviously, WPF possessed a characteristic crystalline region, and the corresponding diffraction peak from the crystalline region occurred at 15.5° and 22.7°, which was attributed to cellulose I crystallinity [18]. No obvious changes of the diffraction peaks occurred when WPF was oxidized to OWPF, which implies that the oxidation mainly occurred in the amorphous region of the WPF [18], only the degree of crystallinity decreased after oxidation [19]. With the increase in the degree of oxidation, the degree of crystallinity of OWPF decreased. This is also in accordance with the morphology observation.

3.1.3. Thermal Stability. Thermogravimetric analysis (TGA) was carried out to evaluate the thermostability of WPF before and after oxidation (shown in Figure 4). WPF showed two mass losses at around 200 and 300°C, related to the amorphous and crystalline region degradation of polysaccharide. OWPF showed main mass losses at around 300°C. The maximum degradation rates were assigned to the degradation of the polysaccharides [11, 20, 21]. It can be seen that, with the increase of oxidation degree, the maximum degradation temperature of the fibers increased from 205 to 322.8°C. Then, with the improved oxidation degree, a slight decrease of the maximum temperature was observed. This may be due to the decline of the amorphous region in WPF during oxidation. The amorphous region of WPF was destroyed, and the proportion of the crystalline region in the fibers increased with an increase in the oxidation degree. The decomposition temperature of the crystalline region is higher than the amorphous region, so the thermal stability of the fibers has an obvious increase after oxidation. The slight decrease is due to the further disintegration of the crystalline structure.

3.2. Characterization of OWPF/TPS Composites

3.2.1. Morphology Analysis. OWPFs with different oxidation degrees were incorporated into the TPS matrix to prepare OWPF/TPS composites. SEM micrographs of the fractured surface of the OWPF/TPS composite are shown in Figure 5. It can be seen that there are no starch granule structures present in the OWPF/TPS phase because native corn starch granules were molten or physically broken up into small fragments under the high shear and temperature conditions with the action of glycerol [14]. When the oxidation degree (the $m(NaIO_4)/m(WPF)$ ratio) was 0.125 and 0.25, the fractured surface of OWPF/TPS composites looks a little rough, and a lot of the rod-like fiber ends are exposed on the surface. With a further increase in the oxidation degree of OWPF, the fracture surface of the composite became smooth as shown in Figures 5(c) and 5(d). As expected, in all TPS composites, OWPF dispersed homogeneously in the TPS matrix, indicating excellent phase compatibility because of their chemical similarities.

3.2.2. Mechanical Property. Figure 6 shows the effect of OWPF with different oxidation degrees on the mechanical properties of OWPF/TPS composites. As shown in the figure, TPS showed poor mechanical properties of tensile strength and elongation at break. When OWPFs with oxidation degrees of 0-0.25 were incorporated, the tensile strength increased from 1.52 to 5.02 MPa, and the elongation at break increased from 89.61 to 103.32%. This mechanical improvement can be attributed to the strong interfacial interactions between OWPF and the TPS matrix. However, when the oxidation degree of OWPF increased from 0.25 to 0.5, the tensile strength of the composites decreased gradually from 5.02 to 1.54 MPa, while the elongation at break increased from 103.32 to 196.35%. The possible explanations for this phenomenon are as follows: (1) The WPF fibers became shorter with an increase of the oxidation degree. (2) The crystalline structure of WPF was damaged during oxidation. The results revealed that the aspect ratio of the fibers have an important effect on the mechanical properties of TPS composites. When the oxidation degree was 0.25, the aspect ratio of OWPF is appropriate and favorable for the mutual entanglement between the fibers and the starch matrix and led to the efficient stress transfer from the matrix to the fillers [22, 23]. The improved mechanical properties were also found in many other researches in which TPS was reinforced with chitin or cellulose nanosize fillers [24–26]. Unlike the results in many other researches, the elongation at break of the composites in this study was also improved with the incorporation of OWPF. This must be attributed to the cross-linking reaction between aldehyde and the hydroxyl group which leads to strong interfacial interaction between OWPF and the TPS matrix.

3.2.3. Thermal Stability. TG and DTG curves of the TPS and OWPF/TPS composites are shown in Figure 7. The weight loss below 200°C for all samples was related to the volatilization of water or glycerol, and the maximum degradation rate was assigned to the degradation of polysaccharides [11, 20, 21]. Overall, the incorporation of WPF into TPS resulted in an increase in the thermal stability of the resulting composites compared with the thermoplastic starch matrix, and the oxidation of WPF significantly improved the thermostability of the composites. This improvement can also be attributed

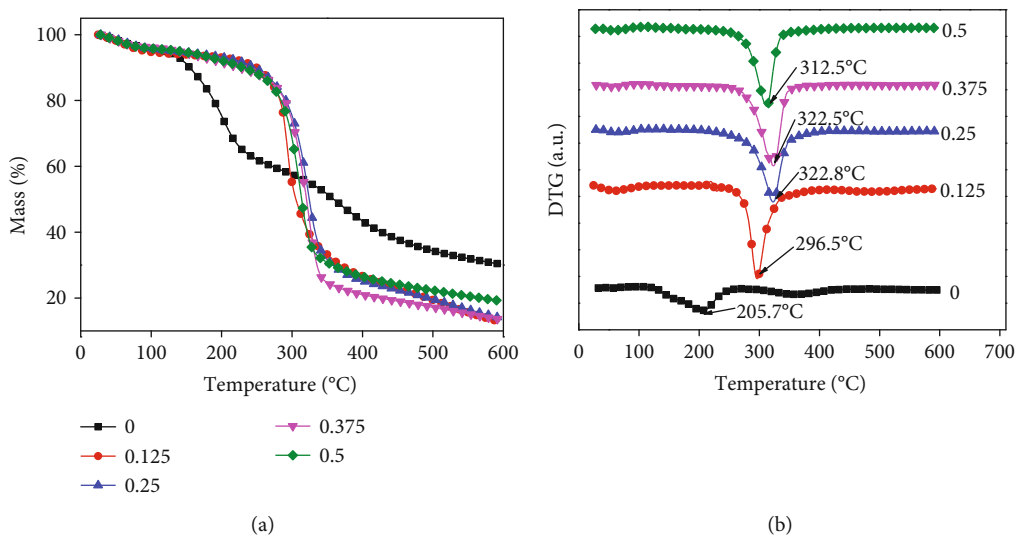

Figure 4: (a) TG curves of OWPF with different degrees of oxidation. (b) DTG curves of OWPF with different degrees of oxidation.

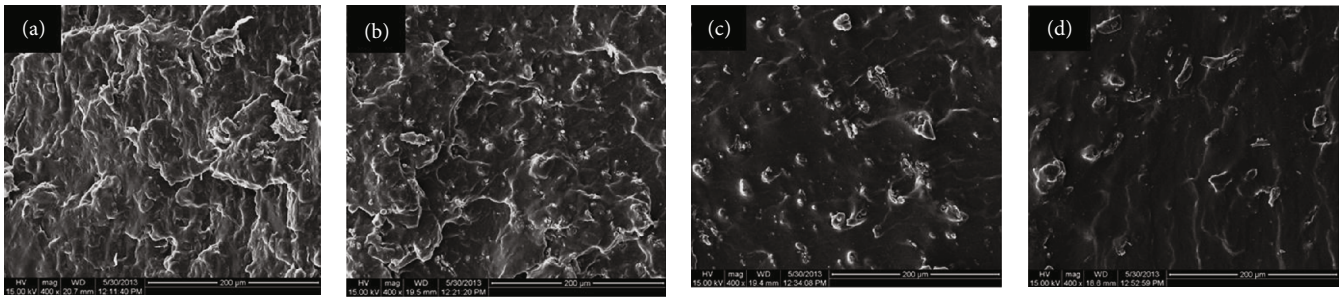

Figure 5: SEM micrographs of the fracture surface of OWPF/TPS composites with different oxidation degrees: (a) 0.125 OWPF/TPS; (b) 0.25 OWPF/TPS; (c) 0.375 OWPF/TPS; (d) 0.5 OWPF/TPS.

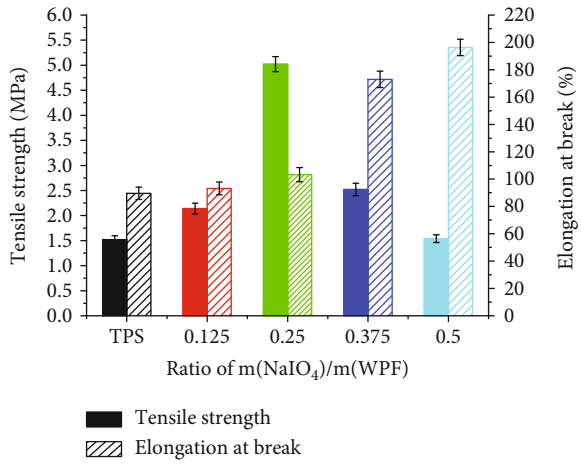

Figure 6: Effect of the oxidation degree of OWPF on tensile strength and elongation at break of OWPF/TPS composites.

to the cross-linking interaction between OWPF and TPS. When the oxidation degree of OWPF surpassed 0.25, the thermal stability of OWPF/TPS composites has a little decrease, which was related to the damage of the crystalline structure of the OWPF during oxidation.

3.2.4. Water Resistance. Water contact angle is one of the important methods for testing the surface wettability of materials, and it is often used as an indicator for the hydrophilicity or hydrophobicity of materials. Figure 8 shows the contact angle of TPS and OWPF/TPS composites, and it can be seen that the contact angle of OWPF/TPS composites was significantly improved compared with TPS. With the increased oxidation degree of WPF, the contact angle of OWPF/TPS composites increased from 79 to 120°. This indicates that the increased aldehyde content in OWPF can promote an effective chemical connection between the aldehyde group and starch macromolecules, thus destroying some of the hydroxyl groups in the starch macromolecules, and thereby reducing the water wettability of the OWPF/TPS composites. The maximum oxidation degree of WPF resulted in the maximum contact angle of the OWPF/TPS composite, all higher than that of the TPS. Therefore, it is possible that the surface water wettability of the OWPF/TPS composites is mainly related to the degree of cross-linking between the

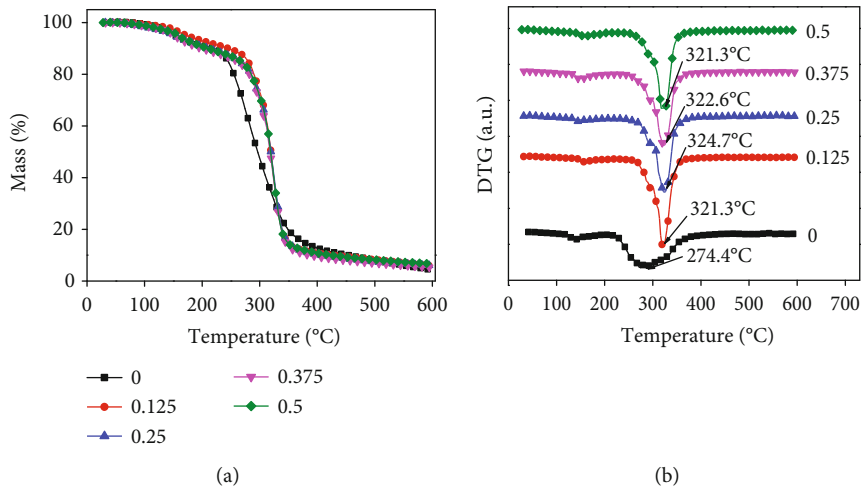

Figure 7: (a)TG curves of OWPF/TPS composites. (b) DTG curves of OWPF/TPS composites.

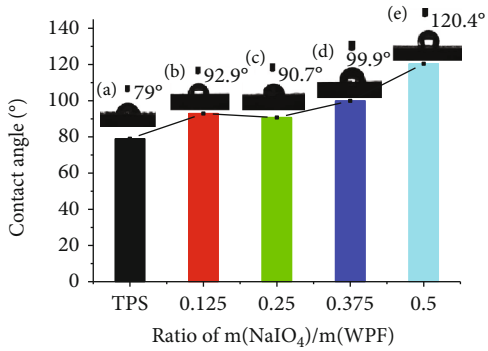

Figure 8: Contact angle of TPS and OWPF/TPS composites: (a) TPS; (b) 0.125 OWPF/TPS; (c) 0.25 OWPF/TPS; (d) 0.375 OWPF/TPS; and (e) 0.5 OWPF/TPS.

OWPF and starch macromolecules, and further characterization will be performed.

4. Conclusions

In this study, an OWPF-reinforced TPS was successfully prepared. The increased oxidization of WPF decreased its aspect ratio, and the tensile strength of OWPF/TPS composites reached a maximum (5.02 MPa) when the oxidation degree of OWPF was 0.25; a higher oxidation degree of OWPF resulted in a smaller OWPF size and a decreased tensile strength of composites. However, the elongation at break of WPF/TPS composites increased with the increased oxidation degree of OWPF. These results can be ascribed to the optimum aspect ratio of OWPF and the chemical bond interaction between OWPF and TPS. In addition, with the increased oxidation degree of OWPF, the water contact angle of OWPF/TPS composites became larger, which was possibly mainly related to the cross-linking between the OWPF and starch macromolecules. This study provided a new way to prepare a degradable TPS composite with satisfying properties to be used for packaging and catering, including for trays, lids, cutlery, cups, and straws.

Data Availability

The data used to support the findings of this study are included within the article.

Conflicts of Interest

The authors declare no conflict of interest.

Authors' Contributions

Peng Yin and Bin Guo conceived and designed the experiments. Wen Zhou and Xin Dong performed the experiments. Yanan Huang significantly contributed materials/reagents/analysis tools. Peng Yin wrote the manuscript, with revisions made by Bin Guo.

Acknowledgments

This work was supported by the Jiangsu Government Scholarship for Overseas Studies, the Natural Science Foundation of Jiangsu Province (Grant No. BK20140967), the National Natural Science Foundation of China (Grant Nos. 20904022 and 20904021), and the Higher School in Jiangsu Province College Students' Practice Innovation Training Programs (Grant No. 201910298025Z).

References

[1] A. Morro, F. Catalina, T. Corrales, J. L. Pablos, I. Marin, and C. Abrusci, "New blends of ethylene-butyl acrylate copolymers with thermoplastic starch. Characterization and bacterial biodegradation," *Carbohydrate Polymers*, vol. 149, pp. 68–76, 2016.

[2] J. Prachayawarakorn, L. Hommanee, D. Phosee, and P. Chairapaksatien, "Property improvement of thermoplastic mung bean starch using cotton fiber and low-density polyethylene," *Starch - Stärke*, vol. 62, no. 8, pp. 435–443, 2010.

[3] J. Prachayawarakorn, P. Sangnitidej, and P. Boonpasith, "Properties of thermoplastic rice starch composites reinforced

by cotton fiber or low-density polyethylene," *Carbohydrate Polymers*, vol. 81, no. 2, pp. 425–433, 2010.

[4] G. Romhány, J. Karger-Kocsis, and T. Czigány, "Tensile fracture and failure behavior of thermoplastic starch with unidirectional and cross-ply flax fiber reinforcements," *Macromolecular Materials and Engineering*, vol. 288, no. 9, pp. 699–707, 2003.

[5] M. G. L. Ramírez, K. G. Satyanarayana, S. Iwakiri, G. B. de Muniz, V. Tanobe, and T. S. Flores-Sahagun, "Study of the properties of biocomposites. Part I. cassava starch-green coir fibers from Brazil," *Carbohydrate Polymers*, vol. 86, no. 4, pp. 1712–1722, 2011.

[6] K. Kaewtatip and J. Thongmee, "Studies on the structure and properties of thermoplastic starch/luffa fiber composites," *Materials & Design*, vol. 40, pp. 314–318, 2012.

[7] H.-M. Park, X. Li, C.-Z. Jin, C.-Y. Park, W.-J. Cho, and C.-S. Ha, "Preparation and properties of biodegradable thermoplastic starch/clay hybrids," *Macromolecular Materials and Engineering*, vol. 287, no. 8, pp. 553–558, 2002.

[8] J. A. Mbey, S. Hoppe, and F. Thomas, "Cassava starch-kaolinite composite film. Effect of clay content and clay modification on film properties," *Carbohydrate Polymers*, vol. 88, no. 1, pp. 213–222, 2012.

[9] H. Schmitt, K. Prashantha, J. Soulestin, M. F. Lacrampe, and P. Krawczak, "Preparation and properties of novel melt-blended halloysite nanotubes/wheat starch nanocomposites," *Carbohydrate Polymers*, vol. 89, no. 3, pp. 920–927, 2012.

[10] P. R. Chang, D. Wu, D. P. Anderson, and X. Ma, "Nanocomposites based on plasticized starch and rectorite clay: structure and properties," *Carbohydrate Polymers*, vol. 89, no. 2, pp. 687–693, 2012.

[11] X. Ma, J. Yu, and J. F. Kennedy, "Studies on the properties of natural fibers-reinforced thermoplastic starch composites," *Carbohydrate Polymers*, vol. 62, no. 1, pp. 19–24, 2005.

[12] J. Prachayawarakorn, P. Ruttanabus, and P. Boonsom, "Effect of cotton fiber contents and lengths on properties of thermoplastic starch composites prepared from rice and waxy rice starches," *Journal of Polymers and the Environment*, vol. 19, no. 1, pp. 274–282, 2011.

[13] A. A. S. Curvelo, A. J. F. de Carvalho, and J. A. M. Agnelli, "Thermoplastic starch-cellulosic fibers composites: preliminary results," *Carbohydrate Polymers*, vol. 45, no. 2, pp. 183–188, 2001.

[14] X. Ma, P. R. Chang, and J. Yu, "Properties of biodegradable thermoplastic pea starch/carboxymethyl cellulose and pea starch/microcrystalline cellulose composites," *Carbohydrate Polymers*, vol. 72, no. 3, pp. 369–375, 2008.

[15] M. Iman and T. K. Maji, "Effect of crosslinker and nanoclay on starch and jute fabric based green nanocomposites," *Carbohydrate Polymers*, vol. 89, no. 1, pp. 290–297, 2012.

[16] Y. M. Zhou, S. Y. Fu, L. M. Zheng, and H. Y. Zhan, "Effect of nanocellulose isolation techniques on the formation of reinforced poly(vinyl alcohol) nanocomposite films," *Express Polymer Letters*, vol. 6, no. 10, pp. 794–804, 2012.

[17] J. Yu, P. R. Chang, and X. Ma, "The preparation and properties of dialdehyde starch and thermoplastic dialdehyde starch," *Carbohydrate Polymers*, vol. 79, no. 2, pp. 296–300, 2010.

[18] L. Shi, W. J. Zhen, and Z. H. Shan, "Preparation and characteristic of dialdehyde cellulose," *Fine Chemicals (China)*, vol. 25, no. 8, pp. 795–798, 2008.

[19] F. R. Tao, D. J. Wang, H. L. Song, and L. J. Chou, "Oxidation of microcrystalline cellulose to oxycellulose by sodium periodate," *Journal of Molecular Catalysis (China)*, vol. 25, no. 2, pp. 119–123, 2011.

[20] A. M. Salaberria, S. C. M. Fernandes, R. H. Diaz, and J. Labidi, "Processing of α-chitin nanofibers by dynamic high pressure homogenization: Characterization and antifungal activity against *A. niger*," *Carbohydrate Polymers*, vol. 116, pp. 286–291, 2015.

[21] M. K. Jang, B. G. Kong, Y. I. Jeong, C. H. Lee, and J. W. Nah, "Physicochemical characterization of α-chitin, β-chitin, and γ-chitin separated from natural resource," *Journal of Polymer Science Part A: Polymer Chemistry*, vol. 42, no. 14, pp. 3423–3432, 2004.

[22] A. M. Salaberria, J. Labidi, and S. C. M. Fernandes, "Chitin nanocrystals and nanofibers as nano-sized fillers into thermoplastic starch-based biocomposites processed by melt-mixing," *Chemical Engineering Journal*, vol. 256, pp. 356–364, 2014.

[23] A. M. Salaberria, R. H. Diaz, J. Labidi, and S. C. M. Fernandes, "Role of chitin nanocrystals and nanofibers on physical, mechanical and functional properties in thermoplastic starch films," *Food Hydrocolloids*, vol. 46, pp. 93–102, 2015.

[24] P. R. Chang, R. Jian, J. Yu, and X. Ma, "Starch-based composites reinforced with novel chitin nanoparticles," *Carbohydrate Polymers*, vol. 80, no. 2, pp. 420–425, 2010.

[25] F. Xie, E. Pollet, P. J. Halley, and L. Averous, "Starch-based nano-biocomposites," *Progress in Polymer Science*, vol. 38, no. 10-11, pp. 1590–1628, 2013.

[26] M. A. S. A. Samir, F. Alloin, and A. Dufresne, "Review of recent research into cellulosic whiskers, their properties and their application in nanocomposite field," *Biomacromolecules*, vol. 6, no. 2, pp. 612–626, 2005.